

Electronic Effects of  $(\text{N}_2\text{S}_2)\text{M}(\text{NO})$  Complexes ( $\text{M} = \text{Fe}, \text{Co}$ ) as Metallodithiolate LigandsJennifer L. Hess,<sup>†</sup> Harold L. Conder,<sup>‡</sup> Kayla N. Green,<sup>†</sup> and Marcetta Y. Darensbourg<sup>\*,†</sup>

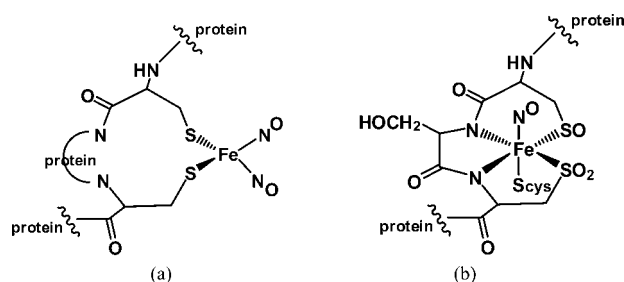
Department of Chemistry, Grove City College, Grove City, Pennsylvania 16127, and Department of Chemistry, Texas A&amp;M University, College Station, Texas 77843

Received September 11, 2007

Heterobimetallic complexes comprised of  $\text{W}(\text{CO})_4$  adducts of  $(\text{N}_2\text{S}_2)\text{M}(\text{NO})$  have been isolated and characterized by  $\nu(\text{CO})$  and  $\nu(\text{NO})$  IR spectroscopies and X-ray diffraction. The molecular structures of  $(\text{N}_2\text{S}_2)\text{M}(\text{NO})$  compounds  $(\text{bme-dach})\text{Co}(\text{NO})$ ,  $[(\text{bme-dach})\text{Co}(\text{NO})]\text{W}(\text{CO})_4$ , and  $[(\text{bme-dach})\text{Fe}(\text{NO})]\text{W}(\text{CO})_4$  [ $\text{bme-dach} = N,N$ -bis(2-mercaptoethyl)-1,4-diazacycloheptane] find the square-pyramidal  $(\text{bme-dach})\text{M}(\text{NO})$  unit to serve as a bidentate ligand via the *cis*-dithiolato sulfurs, with a hinge angle of the butterfly bimetallic structures of ca.  $130^\circ$ . The  $\text{W}(\text{CO})_4$  moiety is used as a probe of the electron-donor ability of the nitrosyl complexes through CO stretching frequencies that display a minor increase as compared to analogous  $[(\text{N}_2\text{S}_2)\text{Ni}]\text{W}(\text{CO})_4$  complexes. These findings are consistent with the electron-withdrawing influence of the  $\{\text{Co}(\text{NO})\}^8$  and  $\{\text{Fe}(\text{NO})\}^7$  units on the bridging thiolate sulfurs relative to  $\text{Ni}^{2+}$ . Also sensitive to derivatization by  $\text{W}(\text{CO})_4$  is the NO stretch, which blue shifts by ca. 30 and  $50\text{ cm}^{-1}$  for the Co and Fe complexes, respectively. Cyclic voltammetry studies find similar reduction potentials ( $-1.08\text{ V}$  vs NHE in *N,N*-dimethylformamide solvent) of the  $(\text{bme-dach})\text{Co}(\text{NO})$  and  $(\text{bme-dach})\text{Fe}(\text{NO})$  free metalloligands, which are positively shifted by ca. 0.61 and 0.48 V, respectively, upon complexation to  $\text{W}(\text{CO})_4$ .

## Introduction

The role of the nitrosyl ligand in bioinorganic and organometallic chemistry continues to develop as its importance in human physiology generates enormous and ever-expanding research endeavors.<sup>1–3</sup> Our work has been to investigate fundamental chemistry relating to dinitrosyliron complexes (DNIC or  $\text{L}_2\text{Fe}(\text{NO})_2$ ) in biological systems such as protein-bound thionitrosyls, for which a prototypical structure is given in Figure 1a.<sup>4–7</sup> Studies of NO transfer from such DNIC moieties have been designed that would take advantage of the potential tetradentate ligating ability



**Figure 1.** (a) Protein-bound  $(\text{Cys})_2\text{Fe}(\text{NO})_2$  DNIC complex. (b) NO-inactivated iron nitrile hydratase enzyme active site, an MNIC complex.<sup>4–7</sup>

provided by the cysteinyl residues in the DNIC, resulting in a mononitrosyl MNIC in an  $\text{N}_2\text{S}_2$  donor set composed of carboxamido nitrogen/cysteine sulfur following an NO transfer reaction.<sup>7</sup> That such a biological binding site for a MNIC is likely has precedence in the nitrile hydratase (NHase) enzyme active site, shown in Figure 1b.<sup>9</sup> In this active site, an iron or a cobalt center is held in a square-

\* To whom correspondence should be addressed. E-mail: marcetta@mail.chem.tamu.edu.

<sup>†</sup> Texas A&M University.

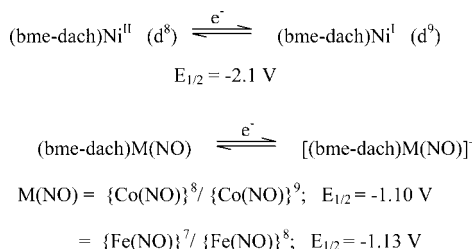
<sup>‡</sup> Grove City College.

- (1) Culotta, E.; Koshland, D. E., Jr. *Science* **1992**, *258*, 1862–1865.
- (2) Scheidt, W. R.; Ellison, M. K. *Acc. Chem. Res.* **1999**, *32*, 350–359.
- (3) Richter-Addo, G. B.; Legzdins, P.; Burstyn, J. *Chem. Rev.* **2002**, *102*, 857–859.
- (4) Vithayathil, A. J.; Temberg, J. L.; Commoner, B. *Nature* **1965**, *207*, 1246–1249.
- (5) Lobysheva, I. I.; Serezhenkov, V. A.; Stucan, R. A.; Bowman, M. K.; Vanin, A. F. *Biochemistry (Moscow)* **1997**, *62*, 801–808.
- (6) Hung, M.-C.; Tsai, M.-C.; Lee, G.-H.; Liaw, W.-F. *Inorg. Chem.* **2006**, *45*, 6041–6047.
- (7) Chiang, C.-Y.; Miller, M. L.; Reibenspies, J. H.; Darensbourg, M. Y. *J. Am. Chem. Soc.* **2004**, *126*, 10867–10874.

(8) Chang, C.-Y.; Darensbourg, M. Y. *J. Biol. Inorg. Chem.* **2006**, *11*, 359–370.

(9) Nagashima, S.; Nakasako, M.; Dohmae, N.; Tsujimura, M.; Takio, K.; Odaka, M.; Yohda, M.; Kamiya, N.; Endo, I. *Nat. Struct. Biol.* **1998**, *5*, 347–351.

**Scheme 1.** Comparisons of the Reduction Potentials of (bme-dach)Ni<sup>II</sup>, (bme-dach)Co(NO), and (bme-dach)Fe(NO)<sup>12–14</sup>

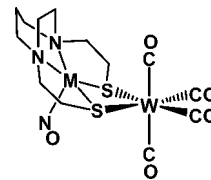


planar contiguous N<sub>2</sub>S<sub>2</sub> arrangement, in which the N<sub>2</sub>S<sub>2</sub> binding motif originates from a cysteine–serine–cysteine tripeptide backbone. While the presence of the NO signifies an inactive form of NHase, NO is endogeneously produced, presumably in the typical manner of the conversion of L-arginine to L-citrulline, which results in NO release.<sup>9,10</sup> Activation of this “as-isolated” form occurs when the NO ligand is removed upon exposure to visible light.<sup>10,11</sup> Also of interest in the NHase active site is the post-translational modification of the cysteinyl sulfurs by oxygenation in a nonsymmetric fashion, resulting in a mixed sulfinato–sulfenato sulfur-donor set along with carboxamido nitrogens.<sup>9,10</sup>

We have explored (N<sub>2</sub>S<sub>2</sub>)M(NO) (M = Co, Fe) complexes that bear similarity in their first coordination sphere to the NHase biological site, where N<sub>2</sub>S<sub>2</sub> = bme-daco (*N,N'*-bis(2-mercaptoethyl)-1,4-diazacycloheptane), designated as ligand **1**, and bme-dach (*N,N'*-bis(2-mercaptoethyl)-1,4-diazacyclooctane), **1'**, respectively.<sup>12</sup> Their characterization was required for studies by Chang et al., who demonstrated that NO transfer from low-molecular-weight DNIC model complexes to biologically relevant targets such as iron and cobalt porphyrins resulted in the formation of such mononitrosyl complexes.<sup>8</sup>

Further elucidation of the properties of these synthetic (N<sub>2</sub>S<sub>2</sub>)M(NO) model complexes uncovered nearly identical one-electron reduction potentials for the (bme-dach)Co(NO) and (bme-dach)Fe(NO) complexes, despite their different Enemark–Feltham electron counts of {Co(NO)}<sup>8</sup> and {Fe(NO)}<sup>7</sup>, respectively (Scheme 1).<sup>13</sup> The former is iso-electronic with Ni<sup>II</sup> (d<sup>8</sup>) and the latter with Ni<sup>III</sup> (d<sup>7</sup>). This interesting concurrence of reduction potentials can possibly be explained by the structures of the nitrosyl complexes, which contain multiple points of electronic buffering, i.e., the M–N–O angle and the degree to which the M is displaced from the N<sub>2</sub>S<sub>2</sub> plane, producing different levels of M–NR<sub>3</sub> and M–SR covalent interactions.<sup>12</sup>

In order to further probe the distinctive electronic properties in such (N<sub>2</sub>S<sub>2</sub>)M(NO) complexes, we have devised a study of such complexes as adducts of W(CO)<sub>4</sub>, the formation



**Figure 2.** Target compound (M = Co, Fe) displaying the W(CO)<sub>4</sub> adduct formed via the bridging dithiolate sulfurs of the (bme-dach)M(NO) metalloligands.

of which ties up or neutralizes the sulfur electron density through thiolate bridging to the metal–carbonyl. Such [(N<sub>2</sub>S<sub>2</sub>)M(NO)]W(CO)<sub>4</sub> complexes would then have two spectroscopic reporters of electron density, the  $\nu(\text{NO})$  and  $\nu(\text{CO})$  vibrational probes. Furthermore, these hetero-bimetallics are of similar structure and geometry to [(N<sub>2</sub>S<sub>2</sub>)Ni]W(CO)<sub>4</sub> complexes, the  $\nu(\text{CO})$  values of which were used to rank the electron-donating ability of *cis*-dithiolate complexes as ligands with classic ligands such as phosphines and diimines.<sup>14,15</sup> The study described herein further explores the electronic character of the (N<sub>2</sub>S<sub>2</sub>)M(NO) complexes and their capability of serving as metalloligands (see Figure 2).

## Experimental Section

**General Methods and Materials.** All solvents used were reagent grade and were purified according to published procedures under an N<sub>2</sub> atmosphere or purified and degassed via a Bruker solvent system.<sup>16</sup> Reagents were purchased from Aldrich Chemical Co. and used as received. While the solid compounds are moderately air-stable, standard Schlenk-line techniques (N<sub>2</sub> atmosphere) and an argon-filled glovebox were used to maintain anaerobic conditions during preparation, isolation, and storage. The (piperidine)<sub>2</sub>W(CO)<sub>4</sub> complex was prepared according to published procedures.<sup>17</sup>

**Physical Measurements.** UV–vis spectra were recorded in CH<sub>2</sub>Cl<sub>2</sub> or *N,N*-dimethylformamide (DMF) on a Hewlett-Packard HP8453 diode array spectrometer. IR spectra were recorded on a Mattson Galaxy series 6021 or on a Bruker Tensor 27 FTIR spectrometer in CaF<sub>2</sub> solution cells of 0.1 mm path length. Mass spectrometry (ESI-MS) was performed by the Laboratory for Biological Mass Spectrometry at Texas A&M University. Elemental analyses were performed by the Canadian Microanalytical Services, Ltd., Delta, British Columbia, Canada. Electron paramagnetic resonance (EPR) spectra were recorded in frozen DMF using a Bruker ESP 300 equipped with an Oxford ER910 cryostat operating at 9 K.

**Cyclic Voltammetry.** Cyclic voltammograms were recorded on a BAS-100A electrochemical analyzer, using procedures identical with those of previous studies.<sup>12</sup> All experiments were performed under an Ar blanket in DMF solutions containing a 0.1 M [*n*-Bu<sub>4</sub>N]BF<sub>4</sub> electrolyte at room temperature and a Ag<sup>0</sup>/AgCl reference electrode. Because the oxidation waves for samples were overlapped with the Cp<sub>2</sub>Fe/Cp<sub>2</sub>Fe<sup>+</sup> couple, Cp<sub>2</sub>\*Fe was used as an internal reference. The reported values are scaled relative to the normal hydrogen electrode (NHE) using Cp<sub>2</sub>Fe/Cp<sub>2</sub>Fe<sup>+</sup> as the standard ( $E_{1/2} = 0.692 \text{ V vs NHE}$ , DMF solvent) such that all values were

(10) Endo, I.; Nokiri, M.; Tsujimura, M.; Nakasako, M.; Nagashima, S.; Yohda, M.; Oda, M. *J. Inorg. Biochem.* **2001**, *83*, 247–253.

(11) Harrop, T. C.; Mascharak, P. K. *Acc. Chem. Res.* **2004**, *37*, 253–260.

(12) Chang, C.-Y.; Lee, J.; Dalrymple, C.; Sarahan, M. C.; Reibenspies, J. H.; Darensbourg, M. Y. *Inorg. Chem.* **2005**, *44*, 9007–9016.

(13) Enemark, J. H.; Feltham, R. D. *Coord. Chem. Rev.* **1974**, *13*, 339–406.

(14) Rampersad, M. V.; Jeffery, S. P.; Golden, M. L.; Lee, J.; Reibenspies, J. H.; Darensbourg, D. J.; Darensbourg, M. Y. *J. Am. Chem. Soc.* **2005**, *127*, 17323–17334.

(15) Rampersad, M. V.; Jeffery, S. P.; Reibenspies, J. H.; Ortiz, C. G.; Darensbourg, D. J.; Darensbourg, M. Y. *Angew. Chem., Int. Ed.* **2005**, *44*, 1217–1220.

(16) Gordon, A. J.; Ford, R. A. *The Chemists' Companion*; Wiley and Sons: New York, 1972; pp 429–436.

(17) Darensbourg, D. J.; Kump, R. L. *Inorg. Chem.* **1978**, *17*, 2680–2682.

**Table 1.** Crystallographic Data for the Complexes

compound	Co-1'(NO)	[Co-1'(NO)]W(CO) <sub>4</sub>	[Fe-1'(NO)]W(CO) <sub>4</sub>
formula	C <sub>9</sub> H <sub>18</sub> CoN <sub>3</sub> O <sub>5</sub> S <sub>2</sub>	C <sub>13</sub> H <sub>18</sub> CoN <sub>3</sub> O <sub>5</sub> S <sub>2</sub> W	C <sub>13</sub> H <sub>18</sub> FeN <sub>3</sub> O <sub>5</sub> S <sub>2</sub> W
fw	307.31	603.20	600.08
temperature (K)	110(2)	293(2)	273(2)
wavelength (Å)	0.710 73	0.710 73	0.710 73
Z	2	4	4
D <sub>calcd</sub> (Mg/cm <sup>3</sup> )	1.666	2.213	2.186
μ (mm <sup>-1</sup> )	1.724	7.523	7.427
cryst syst	triclinic	monoclinic	monoclinic
space group	P $\bar{1}$	P <sub>2</sub> <sub>1</sub> /n	P <sub>2</sub> <sub>1</sub> /n
unit cell			
a (Å)	7.382(2)	7.656(3)	9.8202(6)
b (Å)	8.006(3)	17.397(6)	13.4267(8)
c (Å)	11.854(4)	14.081(5)	13.7282(8)
β (deg)	99.590(6)	105.091(8)	94.0740
V (Å <sup>3</sup> )	612.6(3)	1810.9(11)	1805.53(19)
GOF	1.096	0.763	0.835
R1, wR2 (%) [ <i>I</i> > 2σ( <i>I</i> )]	0.0642, 0.1175	0.0689, 0.1247	0.0687
R1, wR2 (%) (all data)	0.1602, 0.1521	0.1537, 0.1449	0.0775

referenced to Cp\*<sub>2</sub>Fe/Cp\*<sub>2</sub>Fe<sup>+</sup> (*E*<sub>1/2</sub> = -0.564 V vs Cp<sub>2</sub>Fe/Cp<sub>2</sub>Fe<sup>+</sup>) and then corrected to Cp<sub>2</sub>Fe/Cp<sub>2</sub>Fe<sup>+</sup> and reported relative to the NHE.<sup>18</sup>

**Magnetic Susceptibility.** Magnetic susceptibility measurements were determined via the Evans method<sup>19</sup> for paramagnetic substances using a Mercury 300 MHz NMR spectrometer. For (bme-dach)Fe(NO), the solvent used was CD<sub>2</sub>Cl<sub>2</sub>/CH<sub>2</sub>Cl<sub>2</sub>, and for [(bme-dach)Fe(NO)]W(CO)<sub>4</sub>, it was dimethyl sulfoxide (DMSO)-*d*/DMSO.<sup>19–21</sup>

**Preparation of Compounds.** (*N,N'*-Bis(2-mercaptoethyl)-1,4-diazacycloheptane)nitrosylcobalt, (bme-dach)Co(NO) or Co-1'(NO). In a 100 mL Schlenk flask, 0.352 g (0.634 mmol) of [Co(bme-dach)]<sub>2</sub> (synthesized according to published procedures<sup>12,22</sup>) was dissolved in 75 mL of methanol. The solution was heated to 60 °C, at which time the N<sub>2</sub> atmosphere was replaced with NO gas resulting in a color change of the solution from dark green to a dark purple-black. The solvent was removed in vacuo. The resulting precipitate was dissolved in CH<sub>2</sub>Cl<sub>2</sub> and filtered through Celite. Pentane was added to the filtrate, 1:1 by volume, and the mixture was stirred overnight. The mixture was anaerobically filtered to afford 0.224 g (57.5%) of a dark-purple solid. X-ray-quality crystals of (bme-dach)Co(NO) were obtained by slow diffusion of ether into a CH<sub>2</sub>Cl<sub>2</sub> solution of the product at 10 °C. UV–vis spectrum in CH<sub>2</sub>Cl<sub>2</sub> [ $\lambda_{\max}$  ( $\epsilon$ , M<sup>-1</sup> cm<sup>-1</sup>): 268 (8460), 298 (5990), 364 (1740), 635 (341), 657 (250)]. IR (CH<sub>2</sub>Cl<sub>2</sub>):  $\nu$ (NO) 1604 (m) cm<sup>-1</sup>. Anal. Calcd (found): C, 35.15 (35.17); H, 5.86 (5.39); N, 13.67 (13.49).

(*N,N'*-Bis(2-mercaptoethyl)-1,4-diazacycloheptane)nitrosyliron, (bme-dach)Fe(NO) or Fe-1'(NO). This was prepared as previously reported.<sup>12</sup> Additional characterization of this complex was by electronic absorption spectroscopy. UV–vis spectrum in CH<sub>2</sub>Cl<sub>2</sub> [ $\lambda_{\max}$  ( $\epsilon$ , M<sup>-1</sup> cm<sup>-1</sup>): 242 (13 830), 293 (4990), 333 (4530), 345 (4540), 632 (192), 646 (532)].

[(bme-dach)M(NO)]W(CO)<sub>4</sub> Complexes. **a.** [(*N,N'*-Bis(2-mercaptoethyl)-1,4-diazacycloheptane)nitrosylcobalt]tungsten Tetracarbonyl, [(bme-dach)Co(NO)]W(CO)<sub>4</sub>, or [Co-1'(NO)]W(CO)<sub>4</sub>. In a 100 mL Schlenk flask, 0.118 g (0.25 mmol) of (pip)<sub>2</sub>W(CO)<sub>4</sub><sup>17</sup> and 0.0762 g (0.25 mmol) of (bme-dach)Co(NO)

were dissolved in 40.0 mL of CH<sub>2</sub>Cl<sub>2</sub>. The mixture was stirred at 40 °C for 10–15 min. The flask was cooled to room temperature, and the addition of 60 mL of hexanes led to a precipitate that formed over the course of a few hours. The resulting mixture was anaerobically filtered, and the solid was dried in vacuo to produce 0.112 g (75%) of a brown solid. A CH<sub>2</sub>Cl<sub>2</sub> solution of [Co-1'(NO)]W(CO)<sub>4</sub> was layered with ether to obtain X-ray-quality crystals. UV–vis spectrum in DMF [ $\lambda_{\max}$  ( $\epsilon$ , M<sup>-1</sup> cm<sup>-1</sup>): 295 (22 420), 346 (4780), 379 (4590), 600 (696), 629 (107), 636 (56), 655 (787)]. IR (CH<sub>2</sub>Cl<sub>2</sub>):  $\nu$ (NO) 1638 (m) cm<sup>-1</sup>. IR (DMF):  $\nu$ (CO) 1997 (m), 1878 (s), 1851 (s), 1824 (s) cm<sup>-1</sup>. Anal. Calcd (found): C, 24.4 (25.9); H, 3.04 (2.98); N, 6.83 (6.96).

**b.** [(*N,N'*-Bis(2-mercaptoethyl)-1,4-diazacycloheptane)nitrosyliron]tungsten Tetracarbonyl [2], [(bme-dach)Fe(NO)]W(CO)<sub>4</sub> or [Fe-1'(NO)]W(CO)<sub>4</sub>. In a manner similar to that described above, 0.166 g (0.350 mmol) of (pip)<sub>2</sub>W(CO)<sub>4</sub> was mixed with 0.104 g (0.342 mmol) of (bme-dach)Fe(NO), Fe-1'(NO), ultimately producing 0.165 g (80.5%) of a dark-green solid. A CH<sub>2</sub>Cl<sub>2</sub> solution of [Fe-1'(NO)]W(CO)<sub>4</sub> was layered with ether to obtain X-ray-quality crystals. UV–vis spectrum in DMF [ $\lambda_{\max}$  ( $\epsilon$ , M<sup>-1</sup> cm<sup>-1</sup>): 268 (14 510), 362 (2360), 376 (1830), 446 (1320), 486 (1185), 626 (704), 659 (557)]. IR (CH<sub>2</sub>Cl<sub>2</sub>):  $\nu$ (NO) 1697 (m) cm<sup>-1</sup>. IR (DMF):  $\nu$ (CO) 1998 (m), 1880 (s), 1854 (s), 1827 (s) cm<sup>-1</sup>. Anal. Calcd (found): C, 25.8 (26.0); H, 2.86 (3.00); N, 6.49 (7.00).

**X-ray Crystal Structure Determination.** Crystal data and details for data collection and refinement are given in Table 1. X-ray diffraction data were collected on a Bruker SMART CCD-based diffractometer and covered a hemisphere of space upon combination of three sets of exposures. The structures were solved by direct methods. The following programs were used: for data collection and cell refinement, Bruker XSCANS; data reduction, SHELXTL; absorption correction, SADABS; structure solution, SHELXS-97 (Sheldrick); structure refinement, SHELX-97 (Sheldrick); molecular graphics and preparation of material for publication, SHELXTL-Plus, version 5.1 or later (Bruker).<sup>23,24</sup>

## Results and Discussion

**Physical Properties and Structures.** The Co-1'(NO), Fe-1'(NO), [Co-1'(NO)]W(CO)<sub>4</sub>, and [Fe-1'(NO)]W(CO)<sub>4</sub> com-

(18) Connelly, N. G.; Geiger, W. E. *Chem. Rev.* **1996**, *96*, 877–910.

(19) Evans, D. F. *J. Chem. Soc.* **1959**, 2003–2005.

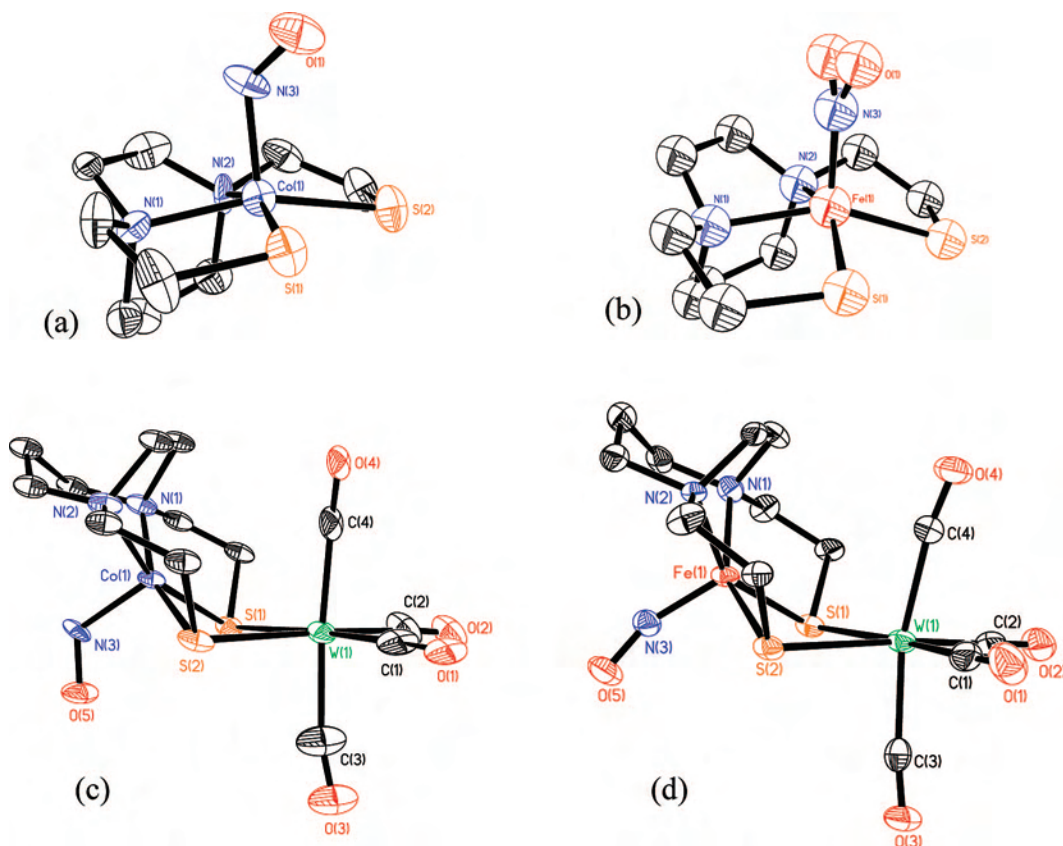
(20) Grant, D. H. *J. Chem. Educ.* **1995**, *72*, 39–40.

(21) Girolami, G. S.; Rauchfuss, T. B.; Angelici, R. J. *Synthesis and Technique in Inorganic Chemistry; A Laboratory Manual*, 3rd ed.; University Science Books: New York, 1999; pp 125–126.

(22) Rabiniwiz, H. N.; Karlin, K. D.; Lippard, S. J. *J. Am. Chem. Soc.* **1976**, *98*, 6951–6957.

(23) SAINT: Program for Reduction of Area Detector Data, 6.63; Bruker AXS Inc.: Madison, WI, 2000; pp 53711–5373.

(24) Sheldrick, G. M. SADABS: Program for Absorption Correction of Area Detector Frames; Bruker AXS Inc.: Madison, WI, 2000; pp 5371–5373.



**Figure 3.** Thermal ellipsoid plots of the molecular structures of (a) (bme-dach)Co(NO) or Co-1'(NO), (b) (bme-dach)Fe(NO) or Fe-1'(NO),<sup>12</sup> (c) [(bme-dach)Co(NO)]W(CO)<sub>4</sub> or [Co-1'(NO)]W(CO)<sub>4</sub>, and (d) [(bme-dach)Fe(NO)]W(CO)<sub>4</sub> or [Fe-1'(NO)]W(CO)<sub>4</sub>, with select atoms labeled and hydrogen atoms omitted.

pounds were isolated as thermally stable (decomposition points at temperatures greater than 200 °C), intensely colored crystalline solids that are moderately air-stable. They degrade over the course of a few days in the absence of a strict anaerobic environment. The Co-1'(NO) and Fe-1'(NO) “free ligand” complexes are highly soluble in CH<sub>2</sub>Cl<sub>2</sub> and DMF and moderately soluble in CH<sub>3</sub>CN; the bimetallics [Co-1'(NO)]W(CO)<sub>4</sub> and [Fe-1'(NO)]W(CO)<sub>4</sub> are highly soluble in DMF, only moderately soluble in CH<sub>2</sub>Cl<sub>2</sub>, and sparingly soluble in CH<sub>3</sub>CN. The cobalt derivatives are both diamagnetic, while Fe-1'(NO) and [Fe-1'(NO)]W(CO)<sub>4</sub> have  $\mu_{\text{obs}}$  values (Evans method) of  $1.6 \pm 0.1$  and  $1.8 \pm 0.1 \mu_{\text{B}}$ , respectively, consistent with the {Fe(NO)}<sup>7</sup> electronic configuration and low-spin iron. IR spectral properties and electrochemical data are presented below.

The paramagnetic Fe-1'(NO) and [Fe-1'(NO)]W(CO)<sub>4</sub> complexes both show a single isotropic signal in their EPR spectra with *g* values of 2.030 and 2.022, respectively. Experimental (frozen DMF solution) and simulated EPR spectra are given in the Supporting Information. The isotropic signal and lack of hyperfine coupling suggest that the unpaired electron of the  $S = 1/2$  systems is delocalized in the {Fe(NO)}<sup>7</sup> unit. The EPR spectrum of Fe-1'(NO) is similar to that previously reported, whose measurement was in CH<sub>2</sub>Cl<sub>2</sub> at 298 K.<sup>12</sup> Interestingly, the isotropic signal in an analogous complex, (bme\*-daco)Fe(NO), where bme\*-daco = *N,N*-bis(2-methyl-2-mercaptoethyl)-1,5-diazacyclooctane, shows distinct hyperfine coupling to <sup>14</sup>N impinged on

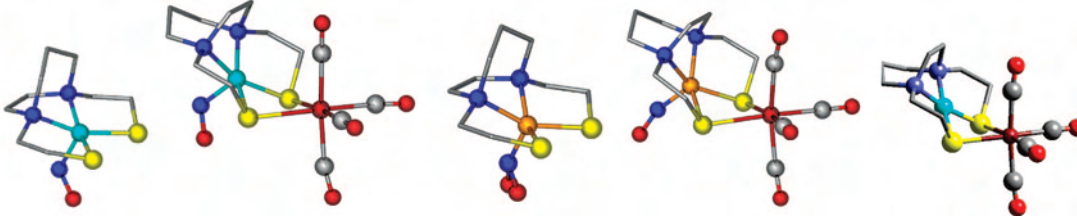
the isotropic signal, as has been seen in (tetraphenylporphyrin)Fe(NO).<sup>25</sup>

The molecular structures of Co-1'(NO), [Co-1'(NO)]W(CO)<sub>4</sub>, and [Fe-1'(NO)]W(CO)<sub>4</sub> were determined by X-ray diffraction analysis; thermal ellipsoid plots are shown in Figure 3. Full structure reports are given in the Supporting Information. Select metric data for Co-1'(NO), [Co-1'(NO)]W(CO)<sub>4</sub>, Fe-1'(NO), and [Fe(bme-dach)NO]W(CO)<sub>4</sub> are presented in Table 2, along with data for the analogous [Ni-1']W(CO)<sub>4</sub> complex.<sup>12,14</sup>

The molecular structures of the [Co-1'(NO)]W(CO)<sub>4</sub>, [Fe-1'(NO)]W(CO)<sub>4</sub>, and [Ni-1']W(CO)<sub>4</sub> complexes are similar in that the connection of the (N<sub>2</sub>S<sub>2</sub>)M unit to W(CO)<sub>4</sub> creates an octahedral geometry at tungsten with S–W–S bite angles of ca. 75° for all. The residual lone pair of each sulfur generates a hinge in the bridge between the two metals whose angle is calculated as the dihedral angle between the N<sub>2</sub>S<sub>2</sub> and S<sub>2</sub>W(CO)<sub>2</sub> best planes. This angle is 127.5° for the Co-1'(NO) and Ni-1' adducts of W(CO)<sub>4</sub> and 121.2° for the Fe-1'(NO) analogue.

As seen in Table 2, the metric parameters of the metallo-ligands change little upon complexation to W(CO)<sub>4</sub>. The most substantial difference occurs for the displacement of cobalt out of the N<sub>2</sub>S<sub>2</sub> plane, which increases by ca. 0.08 Å from the Co-1'(NO) complex, 0.306 Å, to 0.382 Å for the

(25) Wayland, B. B.; Olson, L. W. *J. Am. Chem. Soc.* **1974**, *96*, 6037–6041.

**Table 2.** Selected Bond Distances and Bond Angles of Co-1'(NO), [Co-1'(NO)]W(CO)<sub>4</sub>, Fe-1'(NO), [Fe-1'(NO)]W(CO)<sub>4</sub>, and [Ni-1']W(CO)<sub>4</sub><sup>12,14</sup> (See Figure 3 for Atom Labeling)


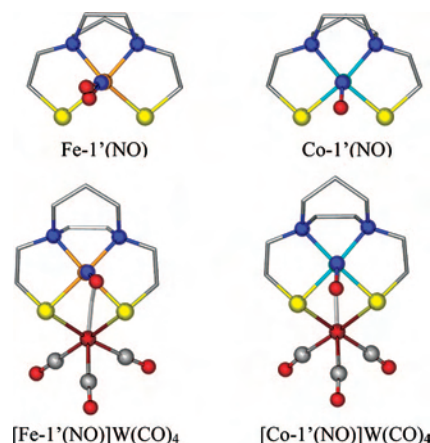
	complex				
	Co-1'(NO)	[Co-1'(NO)]W(CO) <sub>4</sub>	Fe-1'(NO) <sup>8</sup>	[Fe-1'(NO)]W(CO) <sub>4</sub>	[Ni-1']W(CO) <sub>4</sub> <sup>11</sup>
M–W		3.386		3.432	3.249
M–C(4)		3.568		3.834	3.388
M–N (NO)	1.787(7)	1.80(2)	1.705(2)	1.697(8)	
W–C(1)		2.00(2)		1.979(8)	2.03(4)
W–C(2)		2.01(2)		1.938(8)	2.03(8)
W–C(3)		2.05(2)		2.037(8)	1.96(15)
W–C(4)		2.05(2)		2.052(8)	1.96(15)
W–S <sub>avg</sub>		2.586(7)		2.574(2)	2.6(2)
M–S <sub>avg</sub>	2.22(2)	2.224(7)	2.2314(7)	2.26(2)	2.17(16)
M–N <sub>avg</sub> (N <sub>2</sub> S <sub>2</sub> )	1.964(4)	2.00(2)	2.013(2)	2.033(1)	1.93(14)
M–N <sub>2</sub> S <sub>2</sub> disp <sup>a</sup>	0.3063	0.3823	0.5525	0.5498	0.00
C(1)–W–C(2)		85.2(9)		91.0(3)	91(9)
C(3)–W–C(4)		175.5(9)		166.6(3)	172.6(10)
W–C(1)–O(1)		176.0(15)		179.9(9)	174.7(11)
W–C(2)–O(2)		174(2)		173.8(6)	174.9(10)
S(1)–W–S(2)		75.1(1)		75.64(5)	75(8)
S(1)–M–S(2)	96.4(1)	90.2(2)	94.91(3)	88.66(7)	92(9)
N(1)–M–N(2)	80.6(3)	82.2(5)	79.03(9)	79.9(2)	83(7)
M–N–O	123.8(7)	123.1(2)	148(2)	155.4(8)	
dihedral <sup>b</sup>		127.5		121.2	127.5

<sup>a</sup> Displacement of M from the N<sub>2</sub>S<sub>2</sub> best plane. <sup>b</sup> Angle between the N<sub>2</sub>S<sub>2</sub> best plane and the S<sub>2</sub>W(CO)<sub>2</sub> plane.

[Co-1'(NO)]W(CO)<sub>4</sub> complex. In contrast, the same parameter for the Fe-1'(NO) analogue is constant. For both the cobalt and iron derivatives, the S–M–S angle is constricted by ca. 6° upon complexation to the W(CO)<sub>4</sub> unit.

While the M–N–O angle might be expected to respond to the electronic changes occurring at the cobalt or iron center with adduct formation, only minor changes are observed. The Co–N–O angle of 123.8° of Co-1'(NO) is largely the same as that in the W(CO)<sub>4</sub> derivative, 123.1°. For Fe-1'(NO), isomers are found having Fe–N–O angles of 152.4 and 144°, averaging to 148°.<sup>8</sup> There is a minor increase toward linearity in [Fe-1'(NO)]W(CO)<sub>4</sub>: the Fe–N–O angle is 155.4°. The most impressive difference in the “free ligand”, as contrasted to the W(CO)<sub>4</sub>-bound form, is the position of the NO ligand with respect to the unsymmetric diazamesocycle. In the unbound Co-1'(NO) and Fe-1'(NO) units, the NO lies on the two-carbon side of the diazacycloheptane ring while, once bound, it is found on the three-carbon side, with metal displacement from the N<sub>2</sub>S<sub>2</sub> planes toward the NO position accordingly. The reason for this switch is as unclear as the mechanism whereby such isomerism might occur.

There is an apparent preference for the N–O bond vector to eclipse the M–S bond vector in the iron compounds,<sup>12</sup> whereas the N–O bond vectors of the cobalt compounds bisect the two M–S bond vectors both in the tungsten adducts and in the free ligand. This observation is made clearer in the views of the structures shown in Figure 4. Preliminary density functional theory (DFT) calculations have suggested that the orientation of the NO bond vector of Co-1'(NO) does not greatly affect the stability of the



**Figure 4.** “Bird’s eye” view of the M-1'(NO) units in the free metalloligand and in those complexed to W(CO)<sub>4</sub>, focusing on the position of the NO bond vector (the N of NO and the M are eclipsed).

complex because there is no more than a 2 kcal/mol difference between a variety of rotated NO bond vector positions.<sup>26</sup> According to this result, crystal packing forces would be sufficient to control the position of the NO bond vector.

(26) DFT calculations, including geometry optimization, were performed using a hybrid functional (B3LYP) as implemented in *Gaussian '03*. The LANL2DZ basis set was used for cobalt and iron, and the D95 basis set was used for all non-metal atoms. A series of complexes with a NO bond vector in all possible orientations were geometry-optimized. Single-point energies were calculated for both singlet and triplet states of the complexes. The energy differences between all conformations were found to vary no more than 2 kcal/mol. Details and references are given in the Supporting Information.

**Table 3.** Diatomic Ligand IR Data:  $\nu(\text{NO})$  and  $\nu(\text{CO})$  Stretching Frequencies (cm<sup>-1</sup>)<sup>a,b,14</sup>

compound	$\nu(\text{NO})$	$\nu(\text{CO})$			
		$\nu(\text{A}_1^1)$	$\nu(\text{B}_1)$	$\nu(\text{A}_1^2)$	$\nu(\text{B}_2)$
Co-1'(NO)	1603 <sup>b</sup>				
[Co-1'(NO)]W(CO) <sub>4</sub>	1638 <sup>b</sup>	1997m (2002m) <sup>b</sup>	1878s (1889s)	1851s (1844s,br)	1824s (1830s,br)
Fe-1'(NO)	1649 <sup>b</sup>				
[Fe-1'(NO)]W(CO) <sub>4</sub>	1697 <sup>b</sup>	1998 (2004m) <sup>b</sup>	1880 (1892s)	1854 (1846s,br)	1827 (1833s,br)
[Ni-1']W(CO) <sub>4</sub>		1996	1873	1852	1817
[(bme-daco)Ni]W(CO) <sub>4</sub> <sup>c</sup>		1995	1871	1853	1819
[[ema]Ni]W(CO) <sub>4</sub> <sup>2-</sup> (Et <sub>4</sub> N) <sub>2</sub> <sup>c</sup>		1986	1853	1837	1791
(pip) <sub>2</sub> W(CO) <sub>4</sub>		2000	1863	1852	1809

<sup>a</sup> DMF solution spectra except where noted. <sup>b</sup> Spectral measurements in CH<sub>2</sub>Cl<sub>2</sub> solution. <sup>c</sup> bme-daco = 1,5-bis(2-mercaptoethyl)-1,5-diazacyclooctane; ema = *N,N'*-ethylenebis(2-mercaptoacetamide).<sup>14</sup>

**Diatomic Ligand Vibrational Spectroscopy,  $\nu(\text{CO})$  and  $\nu(\text{NO})$ .** The diatomic ligand IR spectra of [Co-1'(NO)]W(CO)<sub>4</sub> and [Fe-1'(NO)]W(CO)<sub>4</sub> were recorded in CH<sub>2</sub>Cl<sub>2</sub> and DMF solvents. The latter gives a better resolution for the  $\nu(\text{CO})$  band; however, the  $\nu(\text{NO})$  band is obscured by the strong absorbance of DMF in the same region. Hence, the  $\nu(\text{NO})$  absorbances are reported as measured in CH<sub>2</sub>Cl<sub>2</sub>.

Four bands assignable to  $\nu(\text{CO})$  are observed in the 1800–2000 cm<sup>-1</sup> range, with patterns similar to those reported for the [(N<sub>2</sub>S<sub>2</sub>)Ni]W(CO)<sub>4</sub> complexes.<sup>14</sup> The absorptions are listed in Table 3 with assignments according to the pseudo-C<sub>2v</sub> symmetry of the W(CO)<sub>4</sub> moiety. For comparison, the  $\nu(\text{CO})$  values of [Ni-1']W(CO)<sub>4</sub>, [(bme-daco)Ni]W(CO)<sub>4</sub>, [[ema]Ni]W(CO)<sub>4</sub><sup>2-</sup>, and (pip)<sub>2</sub>W(CO)<sub>4</sub> are also given. Thus, assuming that the  $\nu(\text{CO})$  values are reporting electron density at the tungsten according to the typical  $\sigma$ -donor/ $\pi$ -back-bonding arguments,<sup>27</sup> the sulfur donors of the metallodithiolate ligands are seen to be better donors to W(CO)<sub>4</sub> than are piperidine ligands of (pip)<sub>2</sub>W(CO)<sub>4</sub>.<sup>14</sup> Furthermore, the electron donor abilities of [Co-1'(NO)] and [Fe-1'(NO)] toward W(CO)<sub>4</sub> are slightly poorer than those of the neutral NiN<sub>2</sub>S<sub>2</sub> complexes, while the dianionic Ni(ema)<sup>2-</sup> ligand appears to transfer most electron density to the W(CO)<sub>4</sub> acceptor.

The  $\nu(\text{NO})$  frequencies of the M–W bimetallic complexes compared to those of the free ligands, Co-1'(NO) and Fe-1'(NO), are also listed in Table 3. As expected, the adduct formation with W(CO)<sub>4</sub> results in a positive shift in the  $\nu(\text{NO})$  values consistent with the withdrawal of electron density from the metallodithiolate ligand. The observation that the  $\nu(\text{NO})$  stretch of Fe-1'(NO) is affected more by W(CO)<sub>4</sub> adduct formation than is that of Co-1'(NO), a positive shift of 48 and 35 cm<sup>-1</sup>, respectively, will be discussed below.

**Electrochemical Studies.** Cyclic voltammograms of Co-1'(NO), Fe-1'(NO), [Co-1'(NO)]W(CO)<sub>4</sub>, and [Fe-1'(NO)]W(CO)<sub>4</sub> were recorded at room temperature in DMF solutions containing 0.1 M [*n*-Bu<sub>4</sub>N][BF<sub>4</sub>]. Selected scans are given in Figure 5, and a summary of the electrochemical data is listed in Table 4.

In general, the [Co-1'(NO)]W(CO)<sub>4</sub> and [Fe-1'(NO)]W(CO)<sub>4</sub> complexes undergo one reversible reduction and one irreversible oxidation, or quasi-reversible as is the case with [Fe-1'(NO)]W(CO)<sub>4</sub>. The former occur at -0.59 and -0.47

V and are assigned to the {Co(NO)}<sup>8/9</sup> and {Fe(NO)}<sup>7/8</sup> redox couples, respectively. The greater ease of reduction in the W(CO)<sub>4</sub> adducts is indicated by the shift to more positive potentials by ca. 0.55 V as compared to the ca. -1.1 V redox events in the free Co-1'(NO) or Fe-1'(NO) ligands. This observation is compatible with the coordination of the W(CO)<sub>4</sub> moiety, which withdraws electron density from the metalloligand via the bridging thiolate sulfurs, resulting in a stabilization of the reduced M(NO) unit.

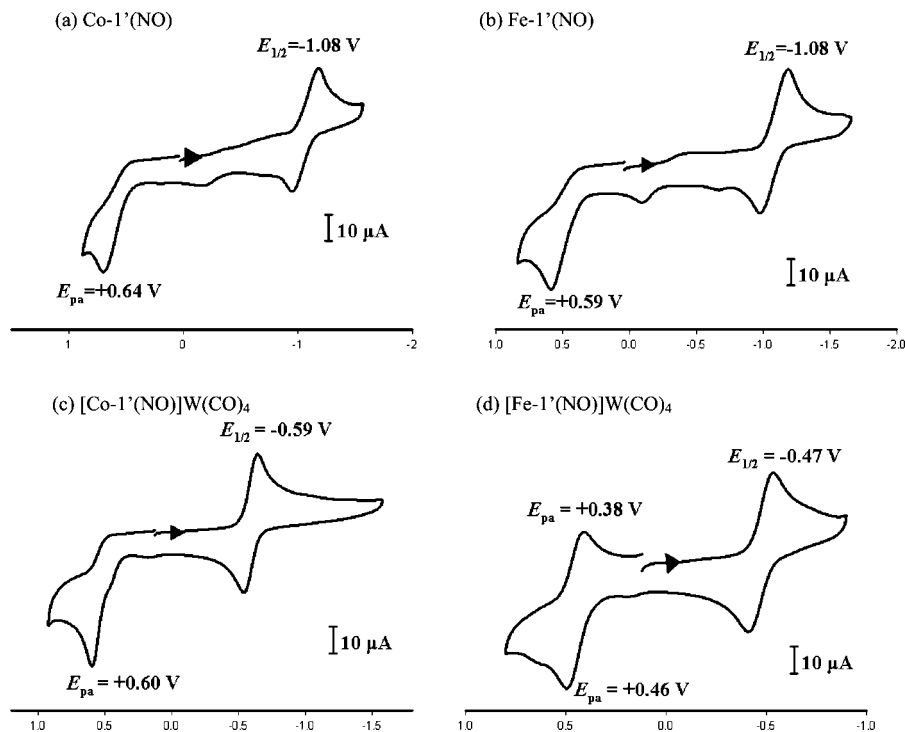
The oxidation events that occur at 0.60 and 0.46 V, respectively, are only slightly shifted (more positively) as compared to the free ligands. Furthermore, when the cyclic voltammogram of the [Co-1'(NO)]W(CO)<sub>4</sub> derivative is initiated at -1.5 V and recorded in the positive direction, two irreversible oxidation events occur, which is likely due to a decomposition product formed at the 0.60 V event. Similarly, there are two additional oxidation events (+0.38 and -0.017 V) in the scan of [Fe-1'(NO)]W(CO)<sub>4</sub> that likely belong to a decomposition product from the 0.46 V event. Highly similar oxidative events with similarly small influences of the W(CO)<sub>4</sub> adduct are seen in the NiN<sub>2</sub>S<sub>2</sub> or Ni-1' complex versus the [Ni-1']W(CO)<sub>4</sub> adduct.<sup>14</sup> These were tentatively assigned to sulfur-based oxidations, and at this point we have no evidence that would confirm or deny this assignment and its validity here. It should be noted that oxidative events appropriate to the W(CO)<sub>4</sub> moiety are not accessible within the scan range.

## Summary and Comments

The overlay of [Co-1'(NO)]W(CO)<sub>4</sub>, [Fe-1'(NO)]W(CO)<sub>4</sub>, and [Ni-1']W(CO)<sub>4</sub> structures (Figure 6) displays similarities between the three structures that originate from the ability of all three metallodithiolates to serve as bidentate sulfur-donor ligands to W(CO)<sub>4</sub> with bite angles of 75°. The graphic also impresses as to the inherent “hinge angle” that originates in the stereochemical effect of the residual lone pair on each sulfur atom donor.<sup>28</sup> A subtle but statistically significant difference in the Co-1'(NO) “free ligand” versus the [Co-1'(NO)]W(CO)<sub>4</sub> adduct is the displacement of cobalt out of the N<sub>2</sub>S<sub>2</sub> best plane by 0.306 and 0.382, respectively. Such differences do not occur in the iron derivatives; however, a difference in the Fe–N–O angle is discernible. We conclude that the electronic effect of engaging the dithiolate as a ligand is experienced through the changes in metal displacement

(27) Crabtree, R. H. *The Organometallic Chemistry of the Transition Metals*, 4th ed.; John Wiley & Sons, Inc.: New York, 2005; pp 88–90.

(28) Hall, M. B. *Inorg. Chem.* **1978**, *17*, 2261–2269.



**Figure 5.** Cyclic voltammograms of DMF solutions of (a) Co-1'(NO), (b) Fe-1'(NO), (c) [Co-1'(NO)]W(CO)<sub>4</sub>, and (d) [Fe-1'(NO)]W(CO)<sub>4</sub> in 0.1 M *n*-Bu<sub>4</sub>NBF<sub>4</sub> with a glassy carbon electrode at a scan rate of 200 mV/s.

**Table 4.** Half-Wave and Anodic Potentials for Reductions and Oxidations of Co-1'(NO), Fe-1'(NO), [Co-1'(NO)]W(CO)<sub>4</sub>, and [Fe-1'(NO)]W(CO)<sub>4</sub> Complexes in a DMF Solvent<sup>a</sup>

compound	$E_{1/2}$ (V) rev. reduction	$E_{pa}$ irr. oxidation
Co-1'(NO)	-1.08	0.64
Fe-1'(NO)	-1.08	0.59
[Co-1'(NO)]W(CO) <sub>4</sub>	-0.59	0.60
[Fe-1'(NO)]W(CO) <sub>4</sub>	-0.47	0.46
Ni-1'	-2.03	0.21
[Ni-1']W(CO) <sub>4</sub>	-1.51	0.30

<sup>a</sup> All potentials were scaled to NHE as referenced to a Cp<sub>2</sub>Fe/Cp<sub>2</sub>Fe<sup>+</sup> standard ( $E_{1/2}^{\text{NHE}} = 0.692$  V; see the Experimental Section). In DMF solutions, a 0.1 M *n*-Bu<sub>4</sub>NBF<sub>4</sub> electrolyte, a glassy carbon working electrode, and a Ag/AgCl reference electrode were used.



**Figure 6.** Overlay of the [Co-1'(NO)]W(CO)<sub>4</sub> (green), [Fe-1'(NO)]W(CO)<sub>4</sub> (blue), and [Ni-1']W(CO)<sub>4</sub> (red) complexes.

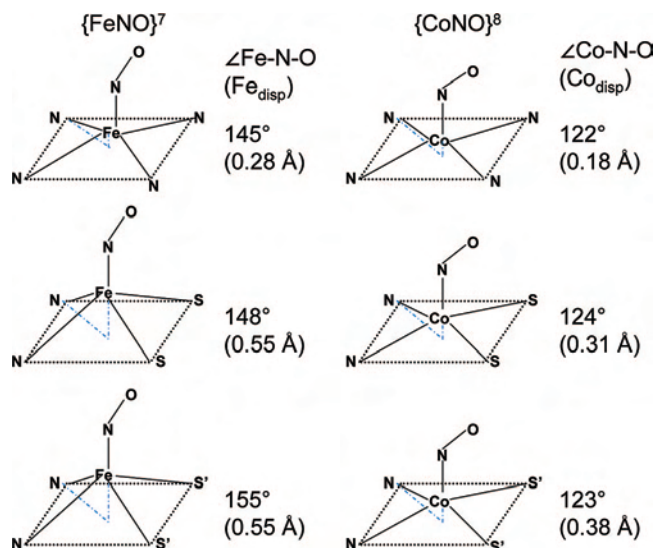
for the Co-1'(NO) complexes, whereas it is evidenced in a small measure through the changes in the M–N–O angles for the Fe-1'(NO) complexes. Such compensating steric features are expected to account for the concurrence of

electrochemical or redox events as measured by cyclic voltammetry.

It is instructive to contrast our square-pyramidal series of (N<sub>2</sub>S<sub>2</sub>)M(NO) complexes with a set of (N<sub>4</sub>)M(NO) complexes (M = Fe, Co) derived from metalloporphyrins.<sup>2</sup> Within an (N<sub>4</sub>)M(NO) series, {M(NO)}<sup>6</sup>, {M(NO)}<sup>7</sup>, and {M(NO)}<sup>8</sup>, there is reported “a systematic variation in the M–N–O angle, M–N(NO) bond length, and metal ion displacement (from the centroid of the N<sub>4</sub> porphyrin donor set)” according to the Enemark–Feltham electronic configuration of the {M(NO)}<sup>*n*</sup> unit, *n* = 6–8.<sup>2</sup> Greater M–N–O linearity correlates with higher oxidation levels of the Fe(NO) units; the linear {Fe(NO)}<sup>6</sup> unit has the greatest displacement (0.34 Å) from the N<sub>4</sub> plane, while in the {Fe(NO)}<sup>7</sup> complex, the deviation is less (0.28 Å). In contrast, {Co(NO)}<sup>8</sup> finds the cobalt almost coplanar (*M*<sub>disp</sub> of 0.18 Å) and the Co–N–O angle is 122° (Chart 1).<sup>2</sup>

In the case of the (N<sub>2</sub>S<sub>2</sub>)M(NO) series (Chart 1), iron displacement from the N<sub>2</sub>S<sub>2</sub> plane (0.55 Å) is much more dramatic than it is in its (N<sub>4</sub>){Fe(NO)}<sup>7</sup> analogue, and neutralization of the thiolate sulfur charge by adduct formation with W(CO)<sub>4</sub> makes little difference. In contrast, the effect of diminishing the sulfur-donor ability to the {Co(NO)}<sup>8</sup> unit by W(CO)<sub>4</sub> adduct formation serves to increase the cobalt displacement out of the N<sub>2</sub>S<sub>2</sub> plane. Because delocalization of electron density and the charge is less in the [Co(NO)] unit than in the [Fe(NO)] unit, there is expected to be a stronger electrostatic interaction between Co<sup>III</sup> and the unfettered thiolate sulfur donors than to iron. Hence, the displacement of cobalt (reasonably assigned to Co<sup>III</sup> in all cases here) out of the N<sub>4</sub>, N<sub>2</sub>S<sub>2</sub> and N<sub>2</sub>S<sub>2</sub>'<sub>2</sub> best

**Chart 1.** Series of  $\{Fe(NO)\}^7$  and  $\{Co(NO)\}^8$  complexes focusing on the M–N–O angle and M ion displacement from the planar ligand donor set.<sup>2</sup> S' indicates modification by  $W(CO)_4$  adduct formation. N<sub>4</sub> = porphyrin.<sup>2</sup>



planes correlates with the increasing soft character of the ligand donor set.

That the ligands transfer substantial electron density to tungsten is evidenced by shifts in the  $\nu(CO)$  and  $\nu(NO)$  stretching frequencies. The former reflects a donor ability of the Co-1'(NO) and Fe-1'(NO) ligands that is better than that of piperidine but poorer than the Ni-1' dithiolate, while the  $\nu(NO)$  values suggest that the M(NO) unit experiences a less negative charge in the bimetallic, accountable to a shift in the thiolate electron density away from the M(NO) units as the  $W(CO)_4$  adduct is formed. Furthermore, electrochemical studies have shown that when bound to  $W(CO)_4$ , the  $[Co(NO)]$  and  $[Fe(NO)]$  moieties are more easily reduced by ca. 0.5 V, as compared to the Co-1'(NO) and Fe-1'(NO) free ligands. While the Ni<sup>II</sup> reduction is significantly more negative in both Ni-1' and  $[Ni-1']W(CO)_4$ , the difference between the reduction events of the free ligand and the adduct is very similar to that of the metal nitrosyl analogues.

The effect of steric and electronic properties of ligands on acceptor metals is typically documented by various spectroscopic techniques that probe changes in the electron distribution about the acceptor metal. The opposite, that is, the changes in the donor ligand as a result of complexation, is less well established. The unique set of ligands that we have studied, containing redox-active metals amenable to solution electrochemistry and, in this case, an additional

reporter unit in the guise of an NO ligand, has permitted a view of electronic shifts from the metalodithiolato ligand resulting from ligation. Such a view of both the acceptor and donor is useful to deconvolute heterobimetallics with bridging thiolate ligands into a donor and an acceptor site. Using these simple systems as models, it is expected that more complicated heteropolymetallics might be better understood. A specific example of a thiolate-bridged biological bimetallic system is the active site of the Acetyl co-A synthase in which a cysteine–glycine–cysteine tripeptide furnishes a Ni<sup>II</sup> binding site and a  $(N_2S_2)Ni$  dithiolate donor to the second nickel, which is catalytically active toward C–C coupling processes.<sup>29</sup> Thiolate-bridged bimetallics are also prominent in the active sites of  $[FeFe]$  and  $[NiFe]$  hydrogenases. The extent to which each monometallic unit participates in donor versus acceptor interactions may be used in the design of small-molecule synthetic analogues for practical use.

**Acknowledgment.** We are grateful for financial support from the National Science Foundation (Grant CHE-0616695) and the R. A. Welch Foundation (Grant A-0924). We also thank the Texas A&M University Chemistry Department's X-ray crystallography facility and Dr. J. H. Reibenspies for his help. We appreciate the assistance of Ryan Bechtold and Stephen Jeffery in the initial stages of this research and of Roxanne Jenkins and Jesse W. Tye for computations as well as the TAMU Chemistry Department and its NSF-REU program in the summer of 2005.

**Supporting Information Available:** X-ray crystallographic data in CIF format and thermal ellipsoid plots and tables containing crystal data and experimental conditions for the X-ray studies, atomic coordinates, and bond lengths and angles for the complexes Co-1'(NO),  $[Co-1'(NO)]W(CO)_4$ , and  $[Fe-1'(NO)]W(CO)_4$ , and details and references for the DFT computations. This material is available free of charge via the Internet at <http://pubs.acs.org>.

IC7017874

- (29) (a) Darnault, C.; Volbeda, A.; Kim, E. J.; Legrand, P.; Vernède, X.; Lindahl, P. A.; Fontecilla-Camps, J. C. *Nat. Struct. Biol.* **2003**, *10*, 271–279. (b) Doukov, T. I.; Iverson, T. M.; Seravalli, J.; Ragsdale, S. W.; Drennan, C. L. *Science* **2002**, *298*, 567–572. (c) Svetlitchnyi, V.; Dobbek, H.; Meyer-Klaucke, W.; Meins, T.; Thiele, B.; Romer, P.; Huber, R.; Meyer, O. *Proc. Natl. Acad. Sci. U.S.A.* **2004**, *101*, 446–451. (d) Seravalli, J.; Xiao, Y.; Gu, W.; Cramer, S. P.; Antholine, W. E.; Krymov, V.; Gerfen, G. J.; Ragsdale, S. W. *Biochemistry* **2004**, *43*, 3944–3955. (e) Webster, C. E.; Darensbourg, M. Y.; Lindahl, P. A.; Hall, M. B. *J. Am. Chem. Soc.* **2004**, *126*, 3410–3411. (f) Amara, P.; Volbeda, A.; Fontecilla-Camps, J. C.; Field, M. J. *J. Am. Chem. Soc.* **2005**, *127*, 2776–2784.